TURBULENT WAKES

E. Baum

TRW Systems Group

Prepared for:

Advanced Research Projects Agency

30 November 1972

SEMI-ANNUAL TECHNICAL REPORT

[illegible]

15 November 1972

Principal Investigator: [illegible] (213) [illegible]

Effective Date of Contract: [illegible] April 1972

Expiration Date: [illegible] 1972

Amount of Contract: $[illegible]

Contract Number: N00014-72-C-[illegible]

Program Code Number: [illegible]

Scientific Officer: Director Fluid Dynamics Programs
[illegible] and Information Sciences Division
Office of Naval Research
Department of the Navy
Arlington, Virginia 22217

Sponsored by
Advanced Research Projects Agency
ARPA Order Number [illegible]

Approved for public release; distribution unlimited.

The views and conclusions contained in this document are those of the authors and should not be interpreted as necessarily representing the official policies, either expressed or implied, of the Advanced Research Projects Agency or the U.S. Government.

TRW

One Space Park

Redondo Beach, California 90278

Unclassified

Security Classification

DOCUMENT CONTROL DATA - R & D

Security classification of title, body of abstract and indexing annotation must be entered when the overall report is classified)

1. ORIGINATING ACTIVITY (Corporate author) TRW Systems Group One Space Park Redondo Beach, California 90278	2a. REPORT SECURITY CLASSIFICATION Unclassified 2b. GROUP

3. REPORT TITLE

Turbulent Wakes

4. DESCRIPTIVE NOTES (*Type of report and, inclusive dates*)

Semi-Annual Technical Report, Period ending 10/31/72

5. AUTHOR(S) (*First name, middle initial, last name*)

6. REPORT DATE November 30, 1972	7a. TOTAL NO. OF PAGES 49	7b. NO. OF REFS 19
8a. CONTRACT OR GRANT NO N00014-72-C-0448 b. PROJECT NO c. d.	9a. ORIGINATOR'S REPORT NUMBER(S) 23023-6001-RU-00 9b. OTHER REPORT NO(S) (*Any other numbers that may be assigned this report*)	

10. DISTRIBUTION STATEMENT

Approved for public release, distribution unlimited

11. SUPPLEMENTARY NOTES	12. SPONSORING MILITARY ACTIVITY ARPA/ONR

13. ABSTRACT

Describes progress in developing turbulence model equations based on an eddy viscosity, written in terms of the scalar quantities e (turbulence energy) and ℓ (integral length scale). The turbulence model equations have been shown to adequately describe mean and turbulence properties for incompressible and compressible flat plate boundary layers. Describes properties of an implicit finite difference method for solving the time-dependent model equations, as applied to laminar (Navier-Stokes) problems. The method appears to be unconditionally stable, of second order accuracy in space and time, and to be very well behaved in the presence of internal shocks.

I

DD FORM 1473 (PAGE 1)

14 KEY WORDS	LINK A		LINK B		LINK C	
	ROLE	WT	ROLE	WT	ROLE	WT
Turbulence modeling						
Time-dependent						
Navier-Stokes equations						
Finite differences						
Alternating-direction implicit						

IIa.

SEMI-ANNUAL TECHNICAL REPORT
TURBULENT WAKES
30 November 1972

Principal Investigator: E. Baum (213) 535-2890

Effective Date of Contract: 1 April 1972

Expiration Date: 31 December 1972

Amount of Contract: $100,000

Contract Number: N00014-72-C-0448

Program Code Number: 2E90

Scientific Officer: Director Fluid Dynamics Programs
Mathematical and Information Sciences Division
Office of Naval Research
Department of the Navy
Arlington, Virginia 22217

Sponsored by
Advanced Research Projects Agency
ARPA Order Number 1801

TRW SYSTEMS GROUP
One Space Park
Redondo Beach, California 90278

TL b

SUMMARY

The objective of this program is to develop the methodology for performing calculations of the turbulent near wake behind a slender body in supersonic flow. The two major technical problems are:

1. To develop turbulence model equations which adequately describe the mean flow properties and, in addition, provide information about the properties of the fluctuation field.

2. To develop numerical procedures for the solution of the model equations.

A turbulence modeling based on an eddy viscosity, which is a function of turbulence properties (the turbulent kinetic energy, e, and an integral scale length function, ℓ), is being developed. The model equations are programmed for solution by a steady state finite difference method (with only the boundary layer form of the laminar and turbulent transport terms included) for comparison with available experimental data. After several modifications of the original equations, the turbulence model has now been shown to adequately describe both mean and turbulence properties of incompressible and compressible adiabatic flat plate boundary layers. Additional verification of the model by comparison with mixing layer experiments would be desirable before applying the model to the near wake calculation.

The near wake problem, because of the recirculation region immediately behind the body, constitutes a boundary value problem. The proposed computational approach is to obtain the steady flowfield as the limit of the time dependent solution of the Navier-Stokes equations with turbulence modeling. The numerical method proposed uses alternating-direction implicit differencing of the conservation form of the equations. The method has been programmed for the laminar Navier-Stokes equations. Truncation error has been shown to be second order in temporal and spatial meshsize. Stability has been demonstrated for a temporal step size up to ten times that beyond which explicit difference methods become unstable. Calculations of shock structure have demonstrated excellent agreement with exact solutions even with relatively poor spatial resolution. Shock jump conditions are accurately calculated even with spatial resolution as poor as half the shock thickness.

An initial application of the numerical methods to the near wake problem, using laminar conservation equations, is in progress.

TABLE OF CONTENTS

1. INTRODUCTION

The principal objective of this program is to develop the capability of performing calculations of turbulent near wakes of slender bodies. Two major subtasks are involved:

1. Develop turbulence model equations applicable to compressible as well as incompressible flows.

2. Develop finite difference methods for the solution of the model equations.

An integral part of the development of the turbulence model equations is comparison of calculations of simple flows with experimental data. Such comparisons are necessary to test the validity of the proposed modeling. These simple flows can be modeled quite adequately using subsets of the complete conservation and turbulence model equations which are being proposed for use in the near wake problem. The particular subset being used for this purpose is one which has been applied to the laminar steady calculation of interacting flows[1], and contains both the complete inviscid terms (in the supersonic flow) and the boundary-layer-like viscous terms. The addition of the turbulence modeling to this existing code and the development and testing of the model equations using this code has been jointly supported by the ROPE Project funded by ABMDA and ARPA under Contract DAHC-60-71-C-0049.

The near wake problem has the intrinsic character of a boundary value problem because of the presence of the subsonic region immediately behind the body. It is possible to make simplifying assumptions in the recirculation region and recast the problem as a pseudo-initial-value-problem. The upstream influence characteristic of the boundary-value-problem is then retained through the presence of an eigenvalue required to pass through a downstream saddle-point singularity (see Reference 1). However, a more rigorous approach (and the one proposed here) is to describe the near wake using the complete steady state conservation equations. The boundary value problem resulting from this formulation can be converted to a more easily solved initial value problem by considering the steady state solution to be the asymptotic limit of a time-dependent calculation. The numerical methods for solution of these equations can be developed relatively independent of

the turbulence modeling, since the laminar (Navier-Stokes) equations embody most of the computational difficulties expected from the complete set of model equations.

This report describes the initial (and relatively independent) work on the modeling of turbulent flows and on the computational techniques required to solve problems described by Navier-Stokes-like equations.

The work described in this report was performed in the period 1 April through 1 October 1972.

2. TURBULENCE MODELING

The calculation of high speed turbulent shear flows requires a description of the Reynolds stresses and the turbulent heat flux terms appearing in the time averaged and hence, mean flow momentum and energy equations. Using arguments similar to those for laminar flows, the transport of momentum and energy by turbulence is found to be proportional to the time averaged rate-of-strain or time averaged temperature gradient, and to the so-called eddy diffusivity function which depends upon the structure of the turbulence, i.e., $\overline{u_i' u_j'} = \varepsilon \left(\frac{\partial \bar{u}_i}{\partial x_j} + \frac{\partial \bar{u}_j}{\partial x_i} \right)$. Classically, the eddy viscosity has been written in terms of mean flow variables which were found by empirical means to represent the turbulence. For example, in simple jets, wakes, and mixing layers, $\varepsilon = K \delta u_{max}$ where K is an empirical constant and δ is the lateral extent of the shearing region. The strong dependence of the classical approach on the geometry of the flow makes it unacceptable for describing a complex turbulent flow configuration such as encountered in the near wake. Instead, a more sophisticated representation of the eddy viscosity based upon a local modeling of the turbulence field is required.

The turbulent field can be represented by as few as two quantities which are generally considered to be the turbulent kinetic energy, $e = \sum_i \overline{u_i' u_i'}/2$ and an integral scale length of the turbulence, ℓ, which is related to the width of the spectrum of the autocorrelation function of the turbulent kinetic energy. The eddy diffusivity, written in terms of these variables is $\varepsilon = \gamma^* e^{1/2} \ell$ where γ^* is a scaling constant. The determination of e and ℓ requires the development of two model equations which describe the convection, production, dissipation, and diffusion of turbulence in the flow. An equation directly describing the turbulent kinetic energy has been used in numerous modern investigations, beginning with Bradshaw[2], is now reasonably well understood and accepted. However, less confidence exists with the second turbulence model equation, primarily because this equation represents a higher order balance between production, dissipation, and diffusion than does the kinetic energy equation. The uncertainties, which exist in the modeling of individual terms, are therefore more

important in the second equation. The determination of the most appropriate second equation is part of the present effort.

Two promising modeling theories for the second turbulence equation have been considered in the present study. One was developed by Saffman[3] in terms of a transport equation for the turbulent vorticity fluctuations, and the other was developed by Jones and Launder[4] who wrote a transport equation for the turbulent energy dissipation rate $\epsilon_d = C_d\, e^{3/2}/\ell$, where C_d is a universal dissipation constant to be determined from experiment. To determine which theory produces better agreement with experiment, both equations were solved, each with the turbulent kinetic energy equation, for a flat plate boundary layer in incompressible flow. These equations are mutually coupled to the mean flow momentum and continuity equations and the resulting solutions, therefore, represent simultaneous solutions of all four equations.

The calculations were initiated by estimating on the basis of experimental data the mean flow velocity profile and the profiles of e and ℓ across the boundary layer. The turbulent boundary layer was then calculated by streamwise marching over a distance of 50 initial boundary layer thicknesses. Experience of other investigators showed initial profile effects to be negligible for an integration of this distance. Referring to the vorticity model of Saffman, by adjusting the constants appearing in the turbulence equations over their acceptable range, it was possible to produce solutions which were in reasonable agreement with experimental data in the law-of-the-wall region. Two such cases are shown in Figure 1 where the velocity ratio $U/U_\tau (U_\tau = (\tau_w/\rho_w)^{1/2})$ is plotted against the reduced coordinate, $y^* = \rho_w u_\tau y/\mu_w$. A wealth of experimental data has been correlated in the law-of-the-wall region with the expression

$$\frac{U}{U_\tau} = C + \frac{1}{\kappa} \ell n\ y^*$$

and the vorticity model results are in reasonable agreement with this correlation with $C = 5.24$ and $\kappa = 0.40$ in the range $100 < y^* < 2000$. However, experimental data by Weighardt[5] is also presented and shows a breakaway from the law-of-the-wall region at about $y^* = 800$, indicative of the outer

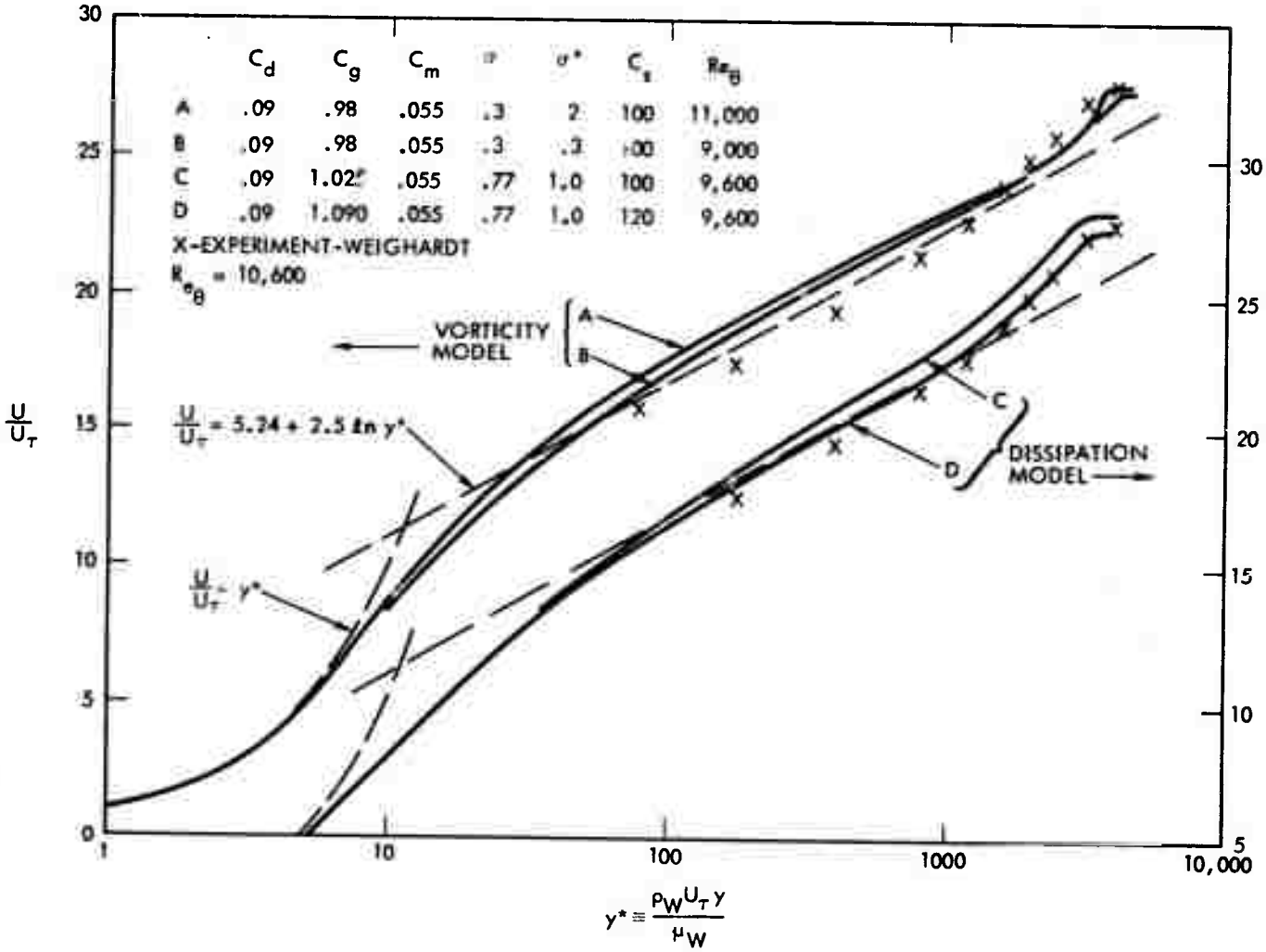

Figure 1. Comparisons with Experiment of Calculated Adiabatic Flat Plate Velocity Profiles at Zero Mach Number

wall-of-the-wake region. The vorticity model thus fails to produce the wall-of-the-wake region of the boundary layer consistent with experiment. This is more clearly seen in Figure 2 where a comparison of one vorticity model solution in velocity defect coordinates can be made with the experimentally correlated velocity defect law. The vorticity model solution does not display the curvature required to agree with the velocity defect law in the wake region ($y/\delta > 0.2$).

Further examination of the solution shows in Figures 3 and 4 that the integral scale length, ℓ/δ, and dimensionless kinematic eddy viscosity $\varepsilon/u_e\delta^*$, where δ^* is the displacement thickness, both reach values in the central portion of the boundary layer which far exceed the measurements of Klebanoff[6] and the values deduced by Maise and McDonald[7] from experimentally measured and correlated velocity profiles. A comparison of the calculated turbulent kinetic energy is made with Klebanoff's data in Figure 5, and the agreement is clearly much better.

Since $\varepsilon \sim e^{1/2}\ell$, the discrepancies noted in Figure 4 between the theoretical (vorticity model) and measured ε are mostly attributable to the length scale, ℓ. This suggests that the problem lies with the vorticity equation. Physically, the difficulty seems to be attributable to the inability of the turbulent vorticity fluctuation function to diffuse from the outer wake region towards the wall; consequently, the wall has much too large an influence in the central portions of the boundary layer.

This calculation was repeated with the energy dissipation rate model equation of Jones and Launder and the results were found to be in acceptable agreement with experimental data. The velocity distribution U/U_τ versus y^* is presented in Figure 1 and clearly displays law-of-the-wall and law-of-the-wake regions which are in good agreement with Weighardt's data, and the correlation curve. Some indication of the sensitivity of the solution to the constants is also given. Curves C and D differ because of a small change in the production constant C_g and sublayer constant C_s.

In Figure 2, the agreement of the velocity profile from the dissipation model with the velocity defect law is excellent, and demonstrates the ability of the theory to predict the law-of-the-wake region. The integral scale length, ℓ/δ, the kinematic eddy viscosity, $\varepsilon/U_e\delta^*$, and the turbulent kinetic

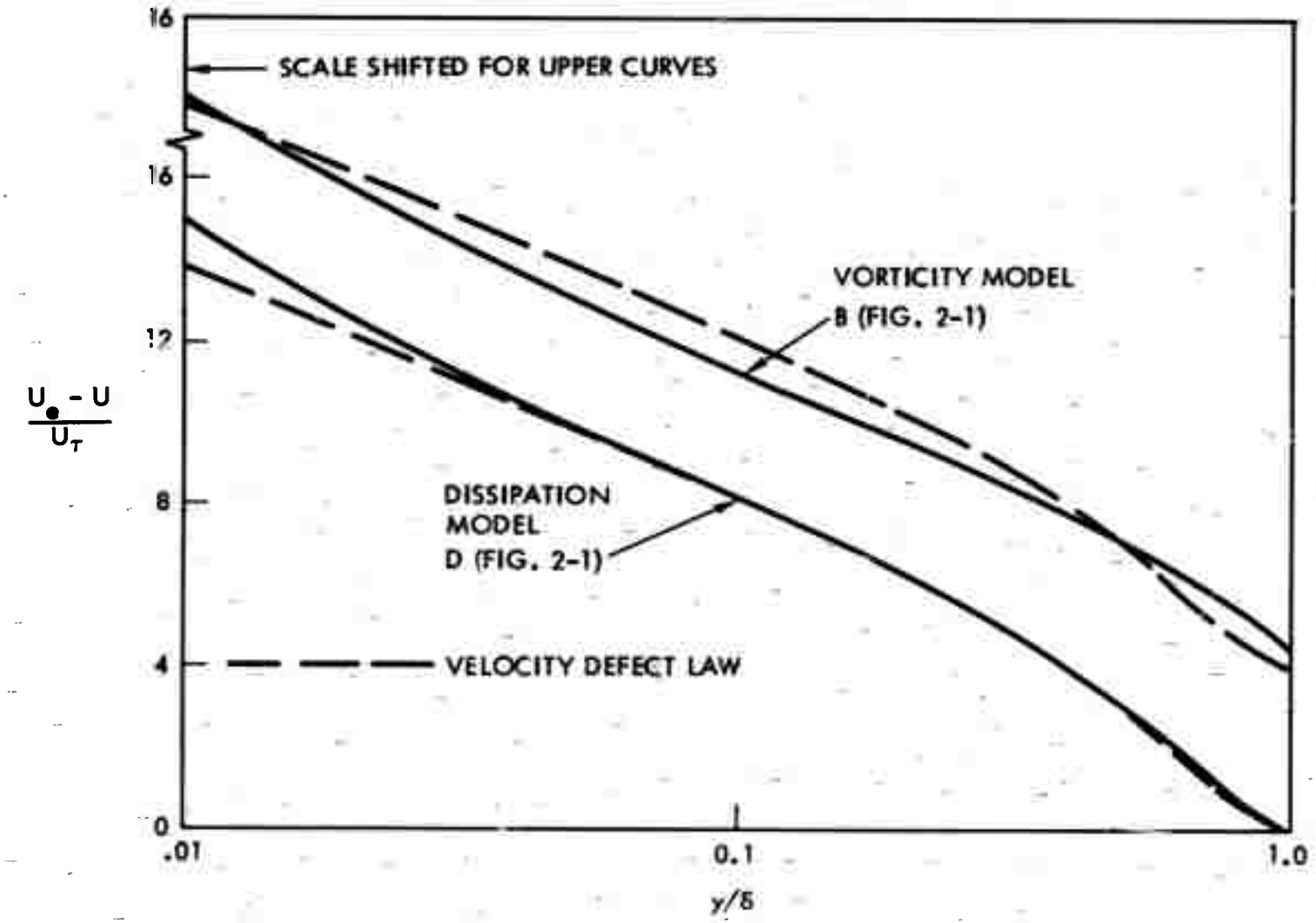

Figure 2. Calculated Adiabatic Flat Plate Velocity Profiles at Zero Mach Number in Velocity Defect Coordinates

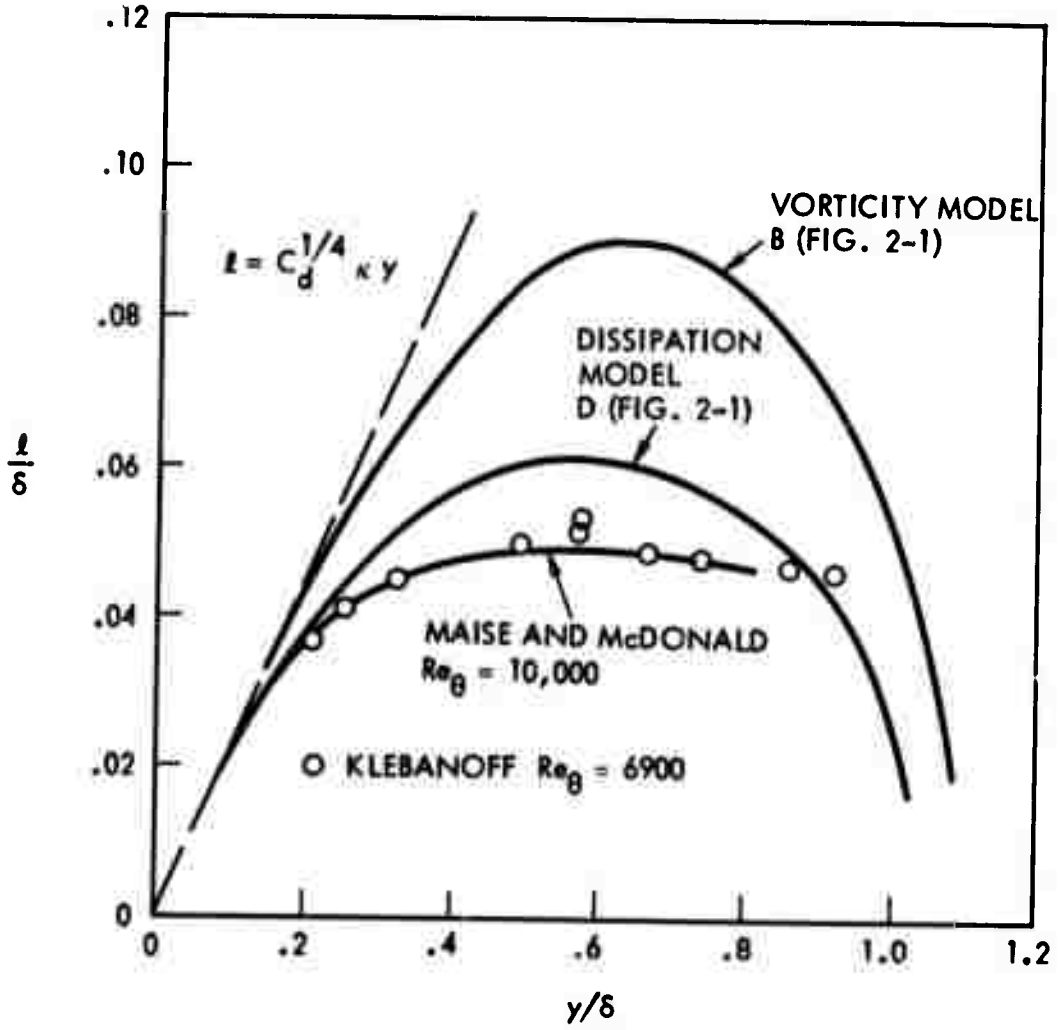

Figure 3. Comparisons with Experiment of Calculated Scale Length Profiles for Mach Zero Adiabatic Flat Plate Flow

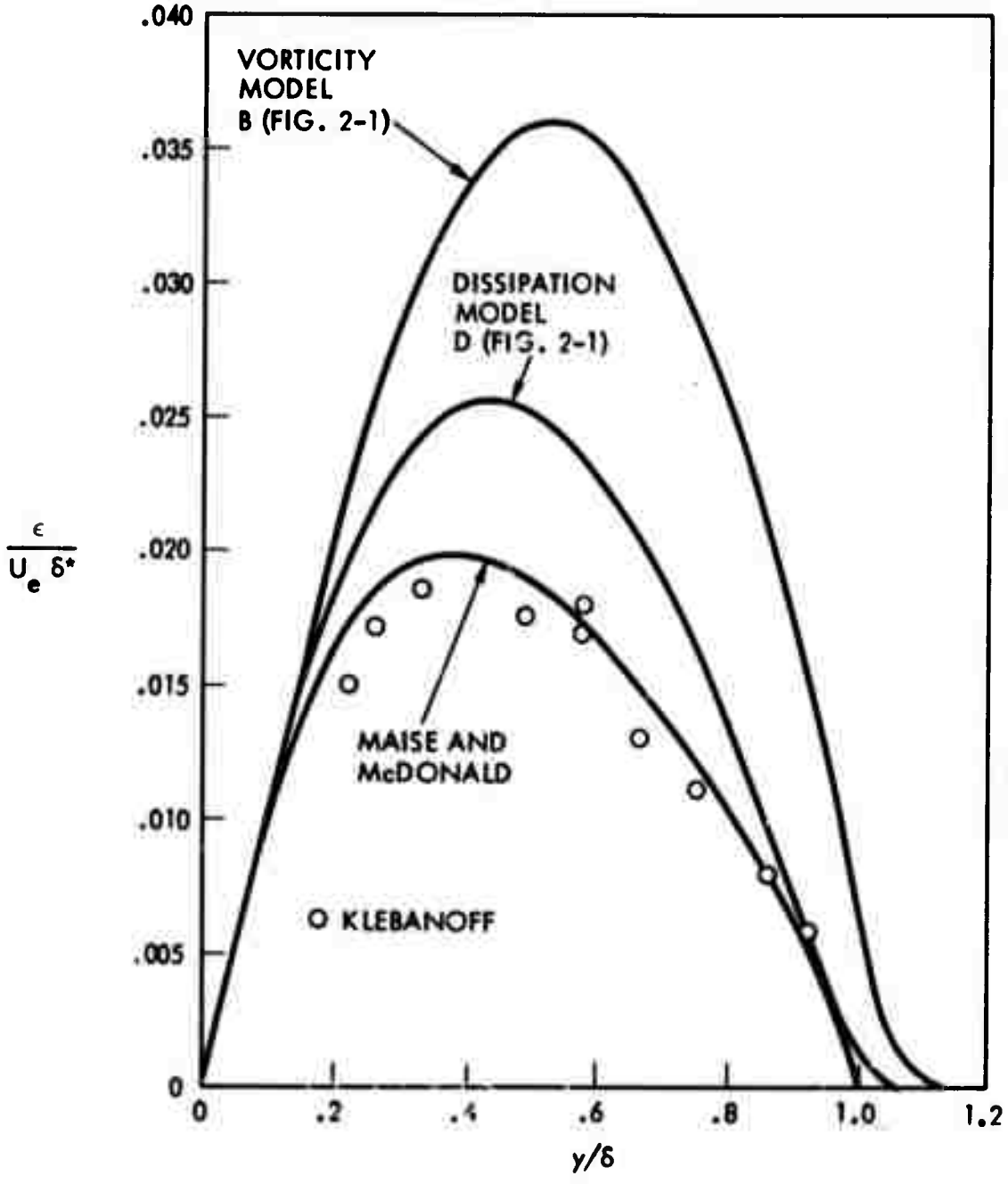

Figure 4. Comparisons with Experiment of Calculated Kinematic Eddy Viscosity Profiles for Mach Zero Adiabatic Flat Plate Flow

energy function, $\sqrt{2e}/U_\tau$, in Figures 3, 4, and 5, respectively, are also in much better agreement with the data, and the differences which are present are not considered serious.

Jones and Launder applied thie dissipation model to accelerating turbulent boundary layers undergoing relaminarization and obtained results which were in remarkably good agreement with existing data. Since an important part of the present task deals with an accelerating boundary layer about the rounded aft shoulder of a reentry vehicle prior to separation, their results are very encouraging. However, an extremely important facet of the modeling is the inclusion of the proper compressibility effects, and hence the next step in the modeling was in this direction.

Two experimentally observed features of compressible turbulent flat plate flow, with which the theoretical model must agree, are that the velocity profile under the transformation $u^* = \int_0^u \left(\frac{\rho}{\rho_e}\right)^{1/2} du$ and the integral length, ℓ, are essentially invariant with Mach number. An analysis of the law-of-the-wall region for compressible flow demonstrated that the two turbulence model equations written for the variables ρe and $\rho^{3/2}\varepsilon_d$ should yield the desired invarience of ℓ with Mach number. This was confirmed in a calculation of a Mach 5 adiabatic boundary layer, and the results are shown in Figure 6 where a comparison with the Mach zero (incompressible case) is made. The results of two other attempts where the variables were e, $\rho^{3/2}\varepsilon_d$, and e, ε_d/ρ are also shown, and are in strong disagreement with the Mach zero results. A comparison of the turbulent kinetic energy with experimental data of Kistler[8] is presented in Figure 7 and shows that acceptable agreement with the variables ρe and $\rho^{3/2}\varepsilon_d$ is achieved. Better agreement is obtained with the variables e and ε_d/ρ, but the large discrepancy in ℓ prohibits use of this function. The effect of Mach number on the eddy viscosity is illustrated in Figure 8, both from the calculation and from the experimentally deduced results of Maise and McDonald. The predicted trend with Mach number is correct even though the values are somewhat larger than the Maise and McDonald results. A comparison of the velocity profiles at Mach 5 and Mach zero is shown in Figure 9 under the

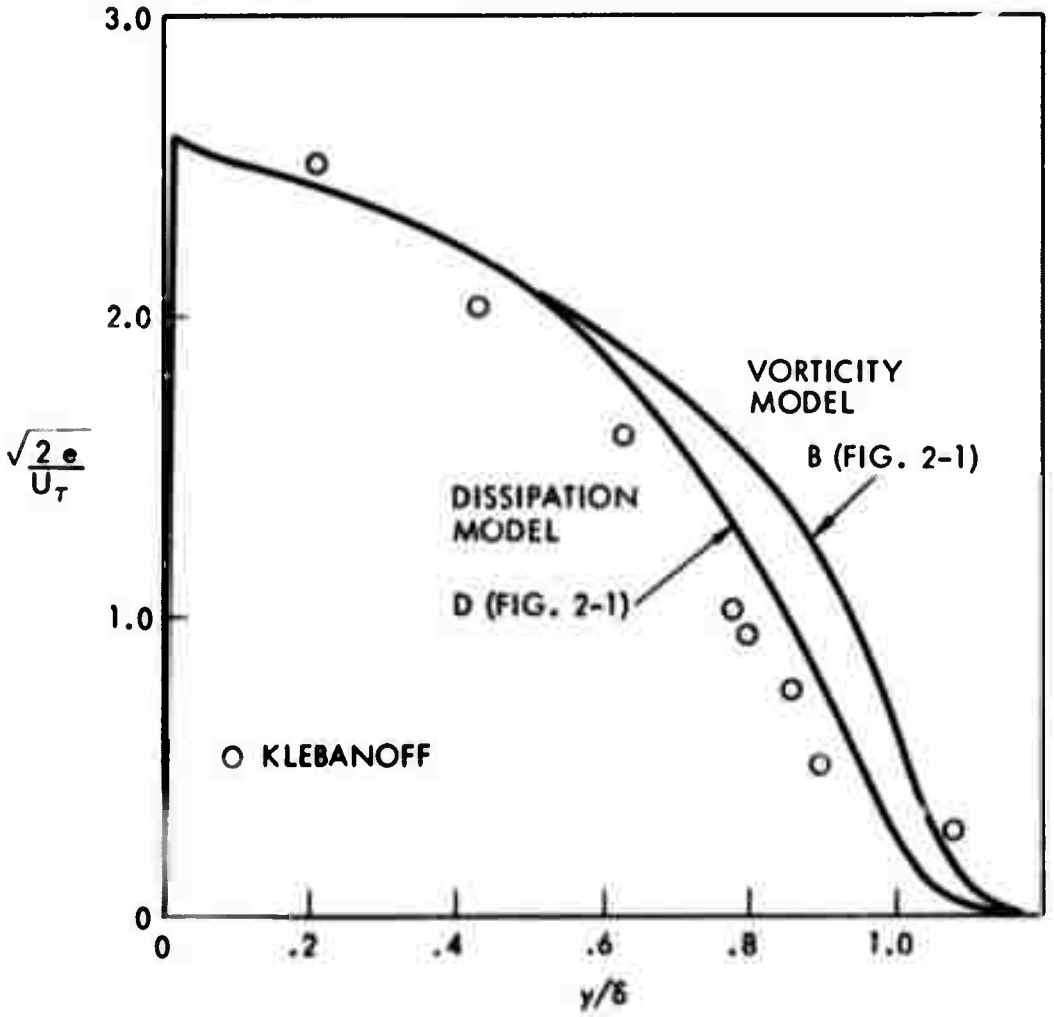

Figure 5. Comparisons with Experiment of Calculated Turbulent Kinetic Energy Profiles for Mach Zero Adiabatic Flat Plate Flow

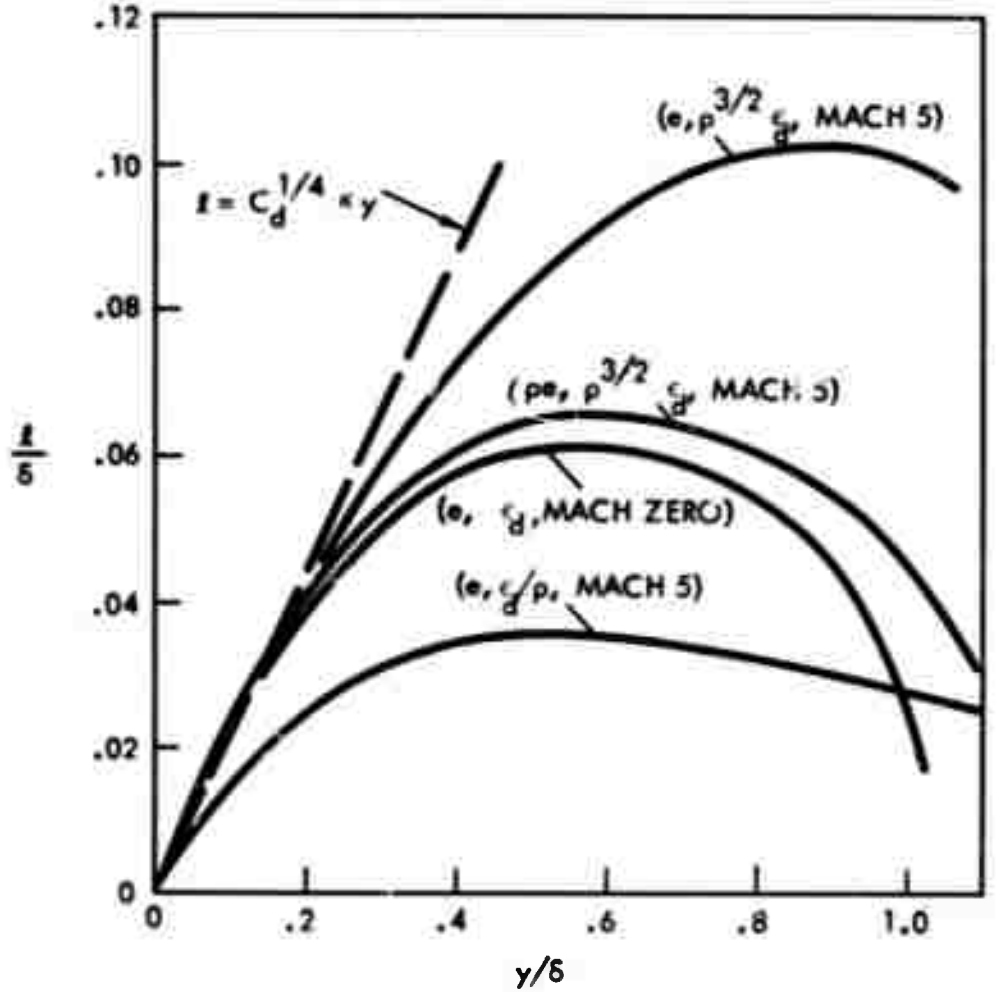

Figure 6. Turbulent Scale Lengths for Different Compressibility Transformations

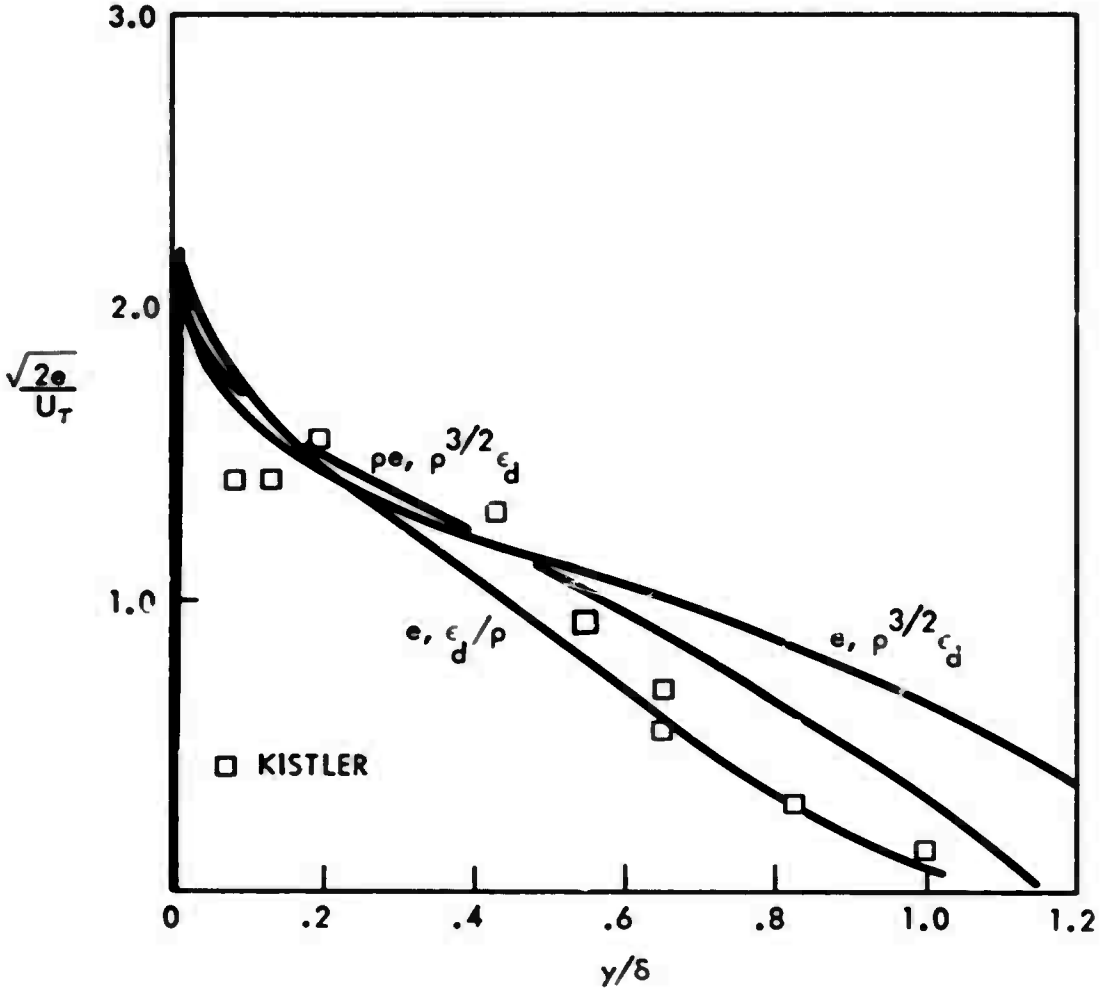

Figure 7. Turbulent Kinetic Energy Profiles for Different Compressibility Transformations

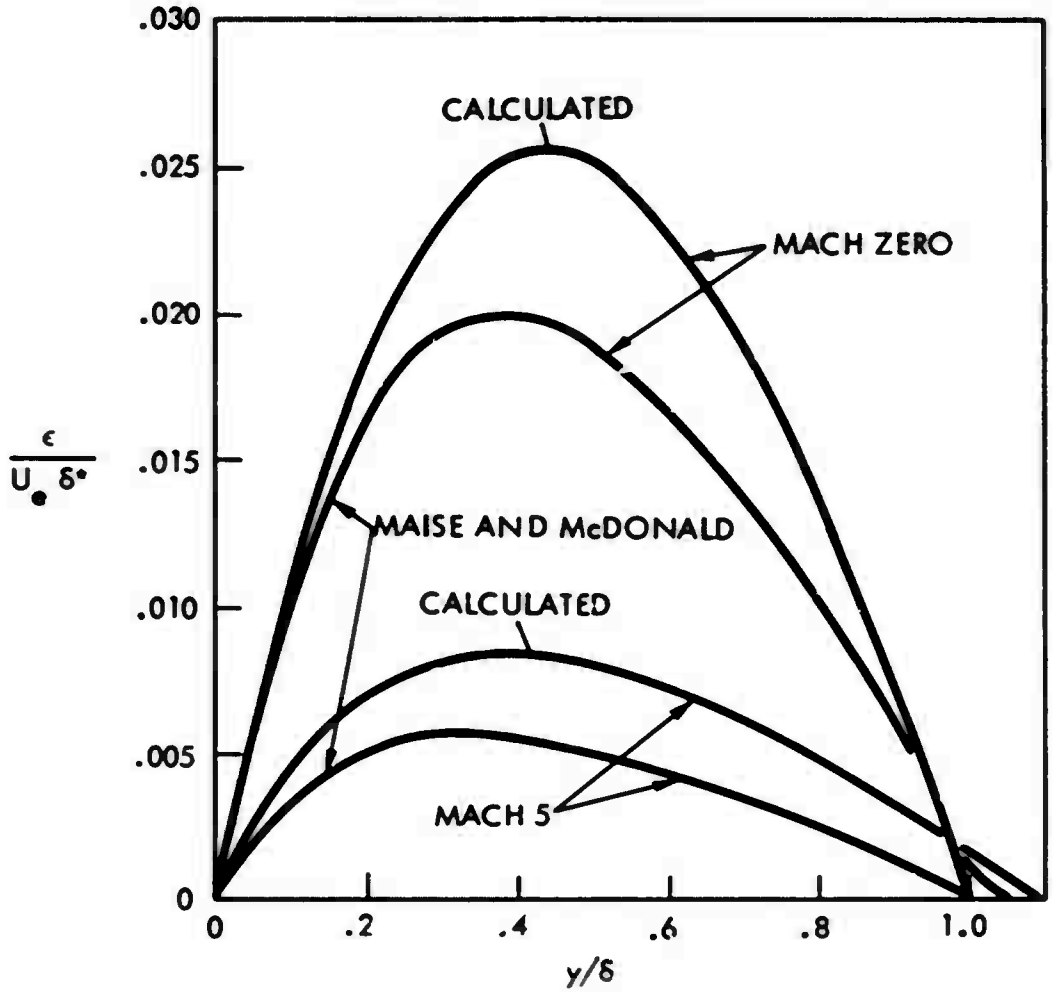

Figure 8. Effect of Mach Number on Eddy Viscosity Dissipation Model ρe, $\rho^{3/2}\epsilon_d$

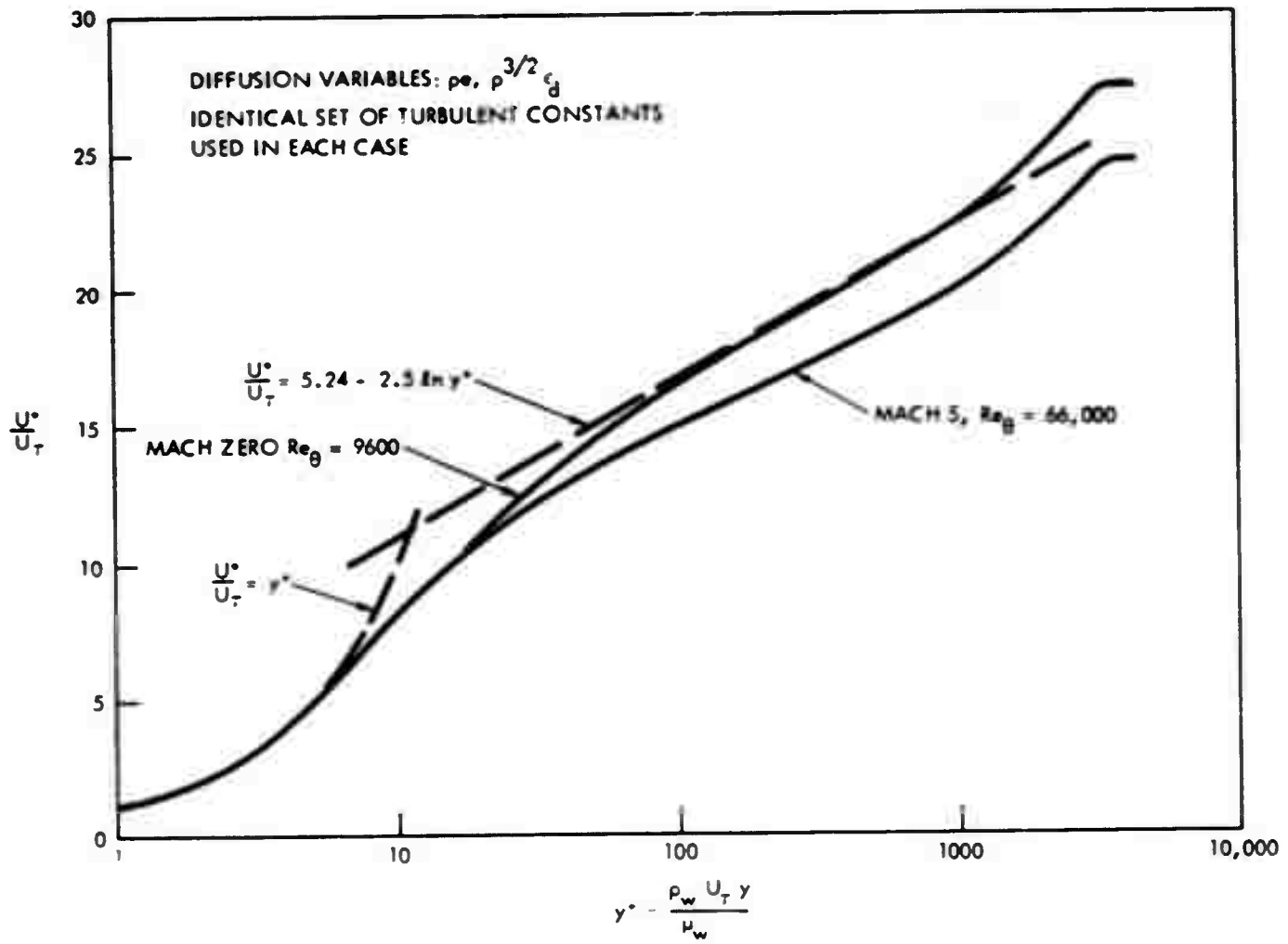

Figure 9. Turbulent Modeling Comparison of Mach 5 and Mach Zero Velocity Profiles Adiabatic Flat Plate

aforementioned transformation. The two curves should be in better agreement; however, the early breakaway of the Mach 5 profile from the laminar sublayer ($y^* \approx 20$) is due to a compressibility effect not accounted for in the sublayer formulation. The turbulent viscosity used in the results shown is modified by the local turbulent Reynolds number $Re_\ell = \rho e^{1/2} \ell / u$ according to

$$\mu_T = \rho e^{1/2} \ell / (1 + .224\ C_s / Re_\ell)$$

Subsequent analysis has shown that the factor $(\rho/\rho_w)^2$ should multiply the constant C_s, and that the effect should be to bring the velocity profile into good agreement with the Mach zero profile. A recalculation of the boundary layer with this minor change is anticipated in the immediate future.

The development of the turbulence modeling has taken several twists and turns, and further comparisons with experiment are yet required. For example, how the modeling holds up under a mixing layer calculation is important to the near wake problem. The decay of the turbulent remnant of the boundary layer is also important during the expansion into the near wake, and it seems likely that additional modifications will be made to improve the model for pressure gradient effects. The turbulence model equations as they stand today are presented below (minus pressure gradient effects). The dissipation rate equation, as given, is the one used to obtain the results presented here.

Turbulent Kinetic Energy Equation

$$\underset{\text{(conv.)}}{\frac{D\rho e}{Dt}} = \underset{\text{(prod.)}}{\mu_T \left(\frac{\partial u}{\partial r}\right)^2} - \underset{\text{(diss.)}}{\rho \varepsilon_d \left(1 + \frac{2}{C_d} \frac{\ell^2}{n^2} \frac{1}{R_\ell}\right)} + \underset{\text{(diff.)}}{\frac{1}{\rho r^\omega} \frac{\partial}{\partial r} \left[\left(\mu + \sigma^* \mu_T\right) r^\omega \frac{\partial \rho e}{\partial r}\right]}$$

Energy Dissipation Rate Equation

$$\underset{\text{(conv.)}}{\frac{D\rho^{3/2}\varepsilon_d}{Dt}} = \underset{\text{(prod.)}}{C_1 \frac{\rho^{1/2}\varepsilon_d}{e} \mu_T \left(\frac{\partial u}{\partial r}\right)^2} - \underset{\text{(diss.)}}{\frac{\rho^{3/2}\varepsilon_d^2}{e} \left(C_2 + \frac{6\ell^2}{C_d^2 n^2} \frac{1}{R_\ell}\right)}$$

$$+ \underset{\text{(diff.)}}{\frac{1}{\rho r^\omega} \frac{\partial}{\partial r} \left[\left(\mu + \sigma\mu_T\right) r^\omega \frac{\partial \rho^{3/2}\varepsilon_d}{\partial r}\right]}$$

where n: distance normal to wall

$$\mu_T = \rho e^{1/2} \ell / (1 + .224\, C_s/R_\ell)$$

$$\varepsilon_d = C_d\, e^{3/2}/\ell$$

$$R_\ell = \rho e^{1/2} \ell / \mu$$

and the constants are:

$C_d = 0.09$ $\qquad$ $C_s = 120$

$C_g = 1.090$ $\qquad$ $\sigma = .77$

$C_m = 0.055$ $\qquad$ $\sigma^* = 1.0$

$C_1 = 2.5 - C_g$ $\qquad$ $C_2 = 2.5 - C_m/C_d$

3. NUMERICAL METHODS

The TACIT (Temporal Alternating-direction-implicit code for Compressible and Incompressible Turbulent flows) code is being developed to solve the complete turbulence model equations. As a first step, the code has been written to solve the compressible time-dependent Navier-Stokes (laminar) equations. This section describes and examines the characteristics of the finite difference methods used.

A number of numerical techniques[9 - 16] have been applied to related problems. With the exception of one method[13], these use explicit difference approximations, which are relatively easy to apply, but which have in common a stability requirement of the form

$$\max [aK_c, bK_R] < 1 \tag{1}$$

where

$$K_c = \frac{(u + c)}{\Delta X} \Delta t \tag{2}$$

$$K_R = \frac{\mu \Delta t}{\rho (\Delta X)^2} \tag{3}$$

a and b are constants of order unity

c = local speed of sound.

This limitation on the time step size makes these methods impractical for low speed flows ($u << c$), where the time interval must be small enough that a sound wave travels less than one spatial mesh interval. For high speed flows, this limitation is not generally as serious, except that high spatial resolution (small ΔX) becomes costly since Δt must then also be reduced. This can become a serious limitation when only limited regions of a flowfield require a small spatial meshsize. This is particularly true of turbulent boundary layers, which require very high resolution for the laminar sublayer.

The one partially implicit scheme[13] which has been applied to related problems is better suited than the explicit methods to low speed flows, but

has stability requirements which make it unsuitable for describing viscous effects at high Reynolds numbers.

A method, which has not been applied to the Navier-Stokes equation, but appears to be well suited for this application for both high and low speed flows, with no stability limitations and reasonably small truncation errors, is the alternating-direction-implicit (ADI) scheme. This method was first applied to the solution of the two-dimensional heat conduction equation

$$\frac{\partial u}{\partial t} = \frac{\partial^2 u}{\partial x^2} + \frac{\partial^2 u}{\partial y^2} \tag{4}$$

by Peaceman and Rachford[17] and to a system of hyperbolic equations of the form

$$\frac{\partial u}{\partial t} = A \frac{\partial u}{\partial x} + B \frac{\partial u}{\partial y} \tag{5}$$

by Gourlay and Mitchell[18], and was shown to be unconditionally stable in both cases. The method would be expected to have the same stability characteristics when applied to the Navier-Stokes equations. The following sections briefly describe the ADI difference approximations and their application to the present problem. A more detailed description will be presented in a forthcoming special report.

3.1 Equations

The TACIT code is designed to solve the continuum conservation equations in rectilinear axisymmetric coordinates. These equations can be written in the form:

continuity

$$\frac{\partial \rho}{\partial t} + \frac{\partial \rho u}{\partial z} + \frac{1}{r} \frac{\partial}{\partial r} (r \rho v) = 0 \tag{6}$$

axial momentum

$$\frac{\partial \rho u}{\partial t} + \frac{\partial \rho u^2}{\partial z} + \frac{1}{r}\frac{\partial}{\partial r}(r\rho uv) + \frac{\partial P}{\partial z} = \frac{\partial \sigma_{zz}}{\partial z} + \frac{1}{r}\frac{\partial}{\partial r}(r\sigma_{rz}) + F_z \tag{7}$$

radial momentum

$$\frac{\partial \rho v}{\partial t} + \frac{\partial \rho uv}{\partial z} + \frac{1}{r}\frac{\partial}{\partial r}(r\rho v^2) + \frac{\partial P}{\partial r} = \frac{\partial \sigma_{rz}}{\partial z} + \frac{1}{r}\frac{\partial}{\partial r}(r\sigma_{rr}) - \frac{\sigma_{\theta\theta}}{r} + F_r \tag{8}$$

total energy

$$\frac{\partial \rho E}{\partial t} + \frac{\partial \rho uH}{\partial z} + \frac{1}{r}\frac{\partial}{\partial r}(r\rho Hv) = \frac{\partial}{\partial z}[-q_z + u\sigma_{zz} + v\sigma_{rz}] + \frac{1}{r}\frac{\partial}{\partial r}[r(-q_r + u\sigma_{rz} + v\sigma_{rr})] + uF_z + vF_r \tag{9}$$

All quantities are non-dimensional, using the following reference values:

$F = \bar{F}L/\rho_r u_r^2$

$E = e + \frac{u^2}{2} + \frac{v^2}{2} = \bar{E}/u_r^2$

$H = h + \frac{u^2}{2} + \frac{v^2}{2} = \bar{H}/u_r^2$ where $h = e + \frac{P}{\rho}$

$q = \bar{q}/\rho_r u_r^3$

$z = \bar{z}/L$

$r = \bar{r}/L$

$t = \bar{t}\, u_r/L$

$\rho = \bar{\rho}/\rho_r$

$u = \bar{u}/u_r$

$v = v/u_r$

$$p = \bar{P}/\rho_r u_r^2$$

$$\sigma = \bar{\sigma}/\rho_r u_r^2$$

The stresses σ_{ij} act on the normal plane i in the direction j. The heat flux q_i is in the direction i. The body force F_i is in the direction i. The energy equation is not completely general, in that radiation is not included; multi-component gases (with or without chemical reactions) are properly described only if all diffusion coefficients are equal and the Lewis number is unity, and if in addition diffusion is due to gradients in species concentration only.

As an initial test of the computing technique, the conservation equations are programmed for solution of a laminar flow, with no body forces present, so that:

$$\sigma_{zz} = \frac{1}{Re}\left\{(2\mu + \lambda)\frac{\partial u}{\partial z} + \frac{\lambda}{r}\frac{\partial}{\partial r}(rv)\right\} \tag{10}$$

$$\sigma_{rr} = \frac{1}{Re}\left\{(2\mu + \lambda)\frac{\partial v}{\partial r} + \lambda\frac{\partial u}{\partial z} + \lambda\frac{v}{r}\right\} \tag{11}$$

$$\sigma_{\theta\theta} = \frac{1}{Re}\left\{(2\mu + \lambda)\frac{v}{r} + \lambda\frac{\partial u}{\partial z} + \lambda\frac{\partial v}{\partial r}\right\} \tag{12}$$

$$\sigma_{rz} = \frac{\mu}{Re}\left\{\frac{\partial v}{\partial z} + \frac{\partial u}{\partial r}\right\} \tag{13}$$

$$-q_z = \frac{\mu}{RePr}\frac{\partial h}{\partial z} \tag{14}$$

$$-q_r = \frac{\mu}{RePr}\frac{\partial h}{\partial r} \tag{15}$$

Finally, it is assumed that an equation of state is available, of the form:

$$\rho = \rho\,(P,h) \tag{16}$$

3.2 Difference Approximations

Two step difference approximations are used, with

$$\left(\frac{\partial A}{\partial t}\right)^{k}_{i,j} = \left(A^{k+1}_{i,j} - A^{k}_{i,j}\right)/\Delta t \tag{17}$$

$$\left(B\,\frac{\partial A}{\partial z}\right)^{k}_{i,j} = B^{k+1}_{i,j}\left(A_{i+1,j} - A_{i-1,j}\right)^{k+1}/2\Delta z \tag{18}$$

$$\left(B\,\frac{\partial A}{\partial r}\right)^{k}_{i,j} = B^{k}_{i,j}\left(A_{i,j+1} - A_{i,j-1}\right)^{k}/2\Delta r \tag{19}$$

$$\left(B\,\frac{\partial A}{\partial z}\right)^{k}_{i+1,j} = B^{k+1}_{i+1,j}\left(\frac{3}{2}A_{i+1,j} - 2A_{i,j} + \frac{1}{2}A_{i-1,j}\right)^{k+1}/\Delta z \tag{20}$$

$$\left(B\,\frac{\partial A}{\partial r}\right)^{k}_{i,j+1} = B^{k}_{i,j+1}\left(\frac{3}{2}A_{i,j+1} - 2A_{i,j} + \frac{1}{2}A_{i,j-1}\right)^{k}/\Delta r \tag{21}$$

$$\left(B\,\frac{\partial A}{\partial z}\right)^{k}_{i-1,j} = B^{k+1}_{i-1,j}\left(-\frac{1}{2}A_{i+1,j} + 2A_{i,j} - \frac{3}{2}A_{i-1,j}\right)^{k+1}/\Delta z \tag{22}$$

$$\left(B\,\frac{\partial A}{\partial r}\right)_{i,j-1} = B^{k}_{i,j-1}\left(-\frac{1}{2}A_{i,j+1} + 2A_{i,j} - \frac{3}{2}A_{i,j-1}\right)^{k}/\Delta r \tag{23}$$

for the first (odd) time step. Here,

$$t^{k+1} = t^{k} + \Delta t$$

$$z_{i\pm1} = z_{i} \pm \Delta z$$

$$r_{j\pm1} = r_{j} \pm \Delta r$$

The even time step approximations are

$$\left(\frac{\partial A}{\partial t}\right)^{k}_{i,j} = \left(A^{k+1}_{i,j} - A^{k}_{i,j}\right)/\Delta t \tag{24}$$

$$\left(B\,\frac{\partial A}{\partial z}\right)^{k}_{i,j} = B^{k}_{i,j}\left(A_{i+1,j} - A_{i-1,j}\right)^{k}/2\Delta z \tag{25}$$

$$\left(B\,\frac{\partial A}{\partial r}\right)^{k}_{i,j} = B^{k+1}_{i,j}\left(A_{i,j+1} - A_{i,j-1}\right)^{k+1}/2\Delta r \tag{26}$$

.
.
.

Here, for the odd step, derivatives in the z direction are implicit (written in terms of dependent variables at the new time point) and derivatives in the r direction are explicit. For the even step, z derivatives are explicit while r derivatives are implicit. When these difference approximations are applied to the Navier-Stokes equations in conservation form, the result is a set of algebraic non-linear equations for values of the dependent variables at time k+1. Coupling between values at i+1, i, i-1 occurs during the odd step so that equations for all values of i are coupled together for any particular value of j, and must, therefore, be solved simultaneously. Conversely, during the even step, the equations for all values of j must be solved simultaneously for any particular value of i. The coupled non-linear algebraic equations are solved by a quasi-linearization technique.

3.3 Truncation Error

Analysis shows that the Navier-Stokes equations, differenced using the approximations of Section 3.2, have a truncation error of order Δt^2, Δz^2, Δr^2. This has been verified for the inviscid terms by performing a calculation in which a spherically symmetric, Gaussian shaped energy pulse is instantaneously introduced into an otherwise uniform very large Reynolds number flow. An analytic solution can be obtained for this problem and the calculated error is indeed second order in Δt, Δz, Δr.

While it is clear that a small truncation error is preferable over a large one, it is usually not obvious how large a truncation error can be tolerated before the solution is unacceptably degraded. In fact, very large truncation errors may be acceptable for problems in which error accumulation is not of overriding importance (such as boundary layer problems, where boundary conditions dominate the solution and the history of the flow, including previously generated errors, becomes progressively less important with distance downstream). On the other hand, wave interaction problems, in which the phase of a wave (which propogates over many wavelengths within the domain) is important, require extremely small truncation errors.

In order to crudely simulate the requirements of the near wake problem, the following problem was numerically solved:

$$t = 0: \quad h = 1 + .005\, e^{-[(z-z_0)^2 + (r-r_0)^2]/4}$$

$$P = \frac{T}{\gamma M_\infty^2} \quad , \quad \rho = 1,\ u = 1,\ v = 0$$

where $$P = \frac{\gamma-1}{\gamma}\rho h \text{ (ideal gas)}$$

$$M = 4,\ Re = 2000$$

For large r_0, this corresponds to an instantaneous cylindrical Gaussian shaped energy pulse at time zero in a Mach 4, otherwise uniform flow. The translational motion can be transformed out so the resulting disturbance

is one-dimensional (cylindrical), centered about the point $r = r_0$, $z = z_0 + t$. Contours of scalar quantities (isotherms, isobars, etc.) are therefore circular in shape, and the degree of distortion of these contours is a quick visual measure of the accumulated errors in the calculation. It was found that $\Delta t = 0.8$, $\Delta z = \Delta r = 1$ produced a solution which is marginally acceptable after 16 time steps ($t = 12.8$). The degradation of this solution with increasing Δt or increasing Δz and Δr is illustrated in Figure 10, which shows contours of $\left(P - \frac{1}{\gamma M_\infty^2}\right)$, the pressure disturbance. The most serious manifestation of accumulating truncation error is the appearance of a wake of error trailing behind the disturbance. This wake consists of cells of alternating sign, with the largest error associated with the cell closest to the disturbance. One cell is added with each time step, so the plot of the solution with the fewest time steps ($\Delta t = 6.4$, two time steps) has an uncluttered appearance, but with large errors.

The conditions of this problem are in some ways more severe than would be encountered in the near wake problem. The spatial resolution of the Gaussian disturbance is quite poor and these conditions would be paralleled in the near wake problem only near the body corner, where a strong expansion produces large gradients, and at the separation and wake shocks. However, these regions are stationary or at most slowly varying with time and can, therefore, be expected to have much smaller temporal contributions to the error.

It appears that doubling Δt or doubling Δz and Δr over the values at the nominal conditions ($\Delta t = 0.8$, $\Delta x = \Delta r = 1$) have a similar effect on the magnitude of the errors. It is reasonable to assume, therefore, that the spatial and temporal contributions to truncation error are of the same order of magnitude under these conditions. For the particular problem being solved, one should expect little further improvement in the solution if only Δt is decreased, leaving Δx and Δr fixed. On the other hand, for a problem which is approaching a stationary state, the temporal contribution to truncation error will decrease considerably, and the time step size can be correspondingly increased without a significant degradation of the solution.

Although it is unrelated to truncation error, it should be noted here that the nominal conditions in Figure 10 ($\Delta t = 0.8$, $\Delta x = \Delta r = 1$) correspond

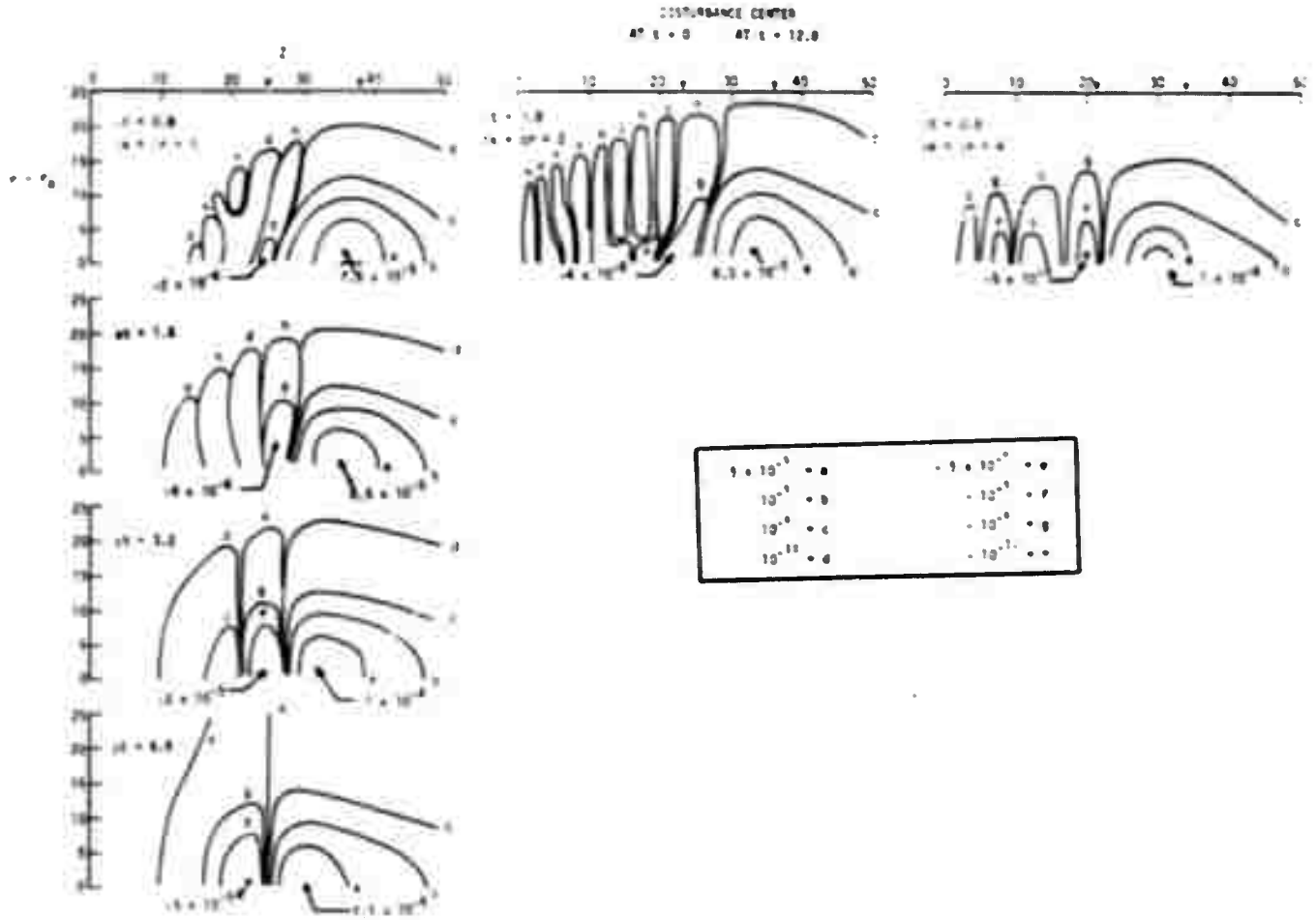

Figure 10. Computed Pressure Contours, $(\bar{P} - \bar{P}_\infty)/(\bar{\rho}_\infty \bar{u}_\infty^2)$: $M_\infty = 4$, Re = 2000, t = 12.8, $r_o = 1000$.

to a Courant number $K_c = 1$. With increasing Δt, K_c ranges from 1 to 8, with no sign of instability. It therefore appears that in the near wake calculation, especially in the later stages as the solution approaches a stationary state, a Courant number considerably greater than unity can be used without serious degradation of the solution due to truncation error.

3.4 Calculation of Shocks

The differencing of the inviscid terms in their conservative form is equivalent to an integration of the differential equation. The integrated conservation equations are, therefore, satisfied even if the detailed profiles between two meshpoints are unresolved. This is most important when internal shocks appear in the domain of the calculation, since the shock jump conditions are then accurately calculated. This property of the method, as well as stability and accuracy characteristics, can be tested by comparing the numerical solution of a normal shock layer problem with the exact solution obtained by G. I. Taylor for the limiting case of infinite Prandtl number.

In this limiting case, the one-dimensional equations in conservation form are given vectorially by

$$\frac{\partial f}{\partial t} + \frac{\partial g}{\partial z} = 0 \tag{27}$$

where

$$f = \begin{bmatrix} \rho \\ \rho u \\ \rho E \end{bmatrix}, \quad g = \begin{bmatrix} \rho u \\ P + \rho u^2 - \sigma_{zz} \\ \rho u H - u\sigma_{zz} \end{bmatrix}$$

with

$$E = H - P/\rho$$

$$\sigma_{zz} = \frac{1}{Re} (2\mu + \lambda) \frac{\partial u}{\partial z}$$

Taylor's exact steady state solution of Equations 27, for an ideal gas equation of state, can be written

$$(a + ku)^A (b - ku) = e^{\beta z} \tag{28}$$

where

$$A = -\left(\frac{\gamma-1}{\gamma+1}\right)\left[1 + \frac{2}{(\gamma-1)M_1^2}\right]$$

$$B = \left(1 - \frac{1}{M_1^2}\right)\left(\frac{mRe}{2\mu + \lambda}\right)$$

$$a = \frac{2 + (\gamma-1)M_1^2}{1 - M_1^2}$$

$$b = \frac{(\gamma+1)M_1^2}{M_1^2-1}$$

$$k = \frac{(\gamma+1)M_1^2}{u_1(M_1^2-1)}$$

u_1 and M_1 are respectively the velocity and Mach number ahead of the shock, while m is the mass flow rate across the shock, ρu. Equation 28 has been normalized in such a way that $u = \frac{u_1 + u_2}{2}$ at $z = 0$.

The one-dimensional version of the differencing presented in Section 3.2 applied to Equations 27 gives difference equations of the form

odd cycle

$$\frac{1}{\Delta t}\left[f^{k+1} - f\right] + \frac{1}{2\Delta z}\left[g_{i+1}^{k+1} - g_{i-1}^{k+1}\right] = 0 \tag{29}$$

even cycle

$$\frac{1}{\Delta t}\left[f^{k+1} - f\right] + \frac{1}{2\Delta z}\left[g_{i+1} - g_{i-1}\right] = 0 \tag{30}$$

where the indices i, k are implied unless otherwise specified.

We observe that the odd cycle is implicit while the even cycle is explicit. The solution of Equation 29 thus requires the quasi-linearization of the non-linear components of the functions f and g; and the solution by iteration of a matrix equation of the type

$$\bar{A}w = \bar{B}$$

where $\bar{A}$ is a band matrix with a width of 11 elements.

The resolution and Courant number effects on the stability and accuracy of the numerical scheme were investigated by solving Equations 29 and 30 to steady state and comparing with Taylor's exact solution.

Some results of calculations of shock structure for M_1 (the Mach number of the undisturbed flow relative to the shock) = 2 are shown in Figures 11 and 12. In Figure 11, the Courant number was fixed at 0.75. The three numerical solutions shown illustrate the effect of spatial resolution. The shock thickness for these conditions corresponds to $\rho_1 u_1 \delta/\mu_1 \approx 10$. The solutions have been shifted in z to give a best fit with the exact solution since the final stationary position of the shock within the calculation domain is not relevant in making these comparisons. The calculation with a spatial meshsize $\rho_1 u_1 \Delta z/\mu_1 = 5.23$ therefore leaves the shock structure entirely unresolved. The jump conditions in velocity (and those in the other flow variables which are not presented here) are nevertheless accurately computed. The shock structure is already represented reasonably well when the mesh spacing is halved to 2.62. The undershoot in velocity at the downstream edge of the shock, which is often observed in other finite difference methods and can be quite large, is not significant here.

In Figure 12, the resolution has been fixed at $\rho_1 u_1 \Delta z/\mu_1 = 1.31$. The time stepsize has been varied to examine the effect of Courant number on stability. The calculation was found to be stable even for a Courant number as large as 10. The temporal truncation error associated with this large time step size apparently does not prevent the approach to a steady solution. Since it is likely that an oscillatory or divergent solution which fails to to approach a steady state would result when the time step size becomes large enough that the temporal truncation error dominates the solution, it can be assumed that the temporal truncation error is still reasonably small even with this large step size.

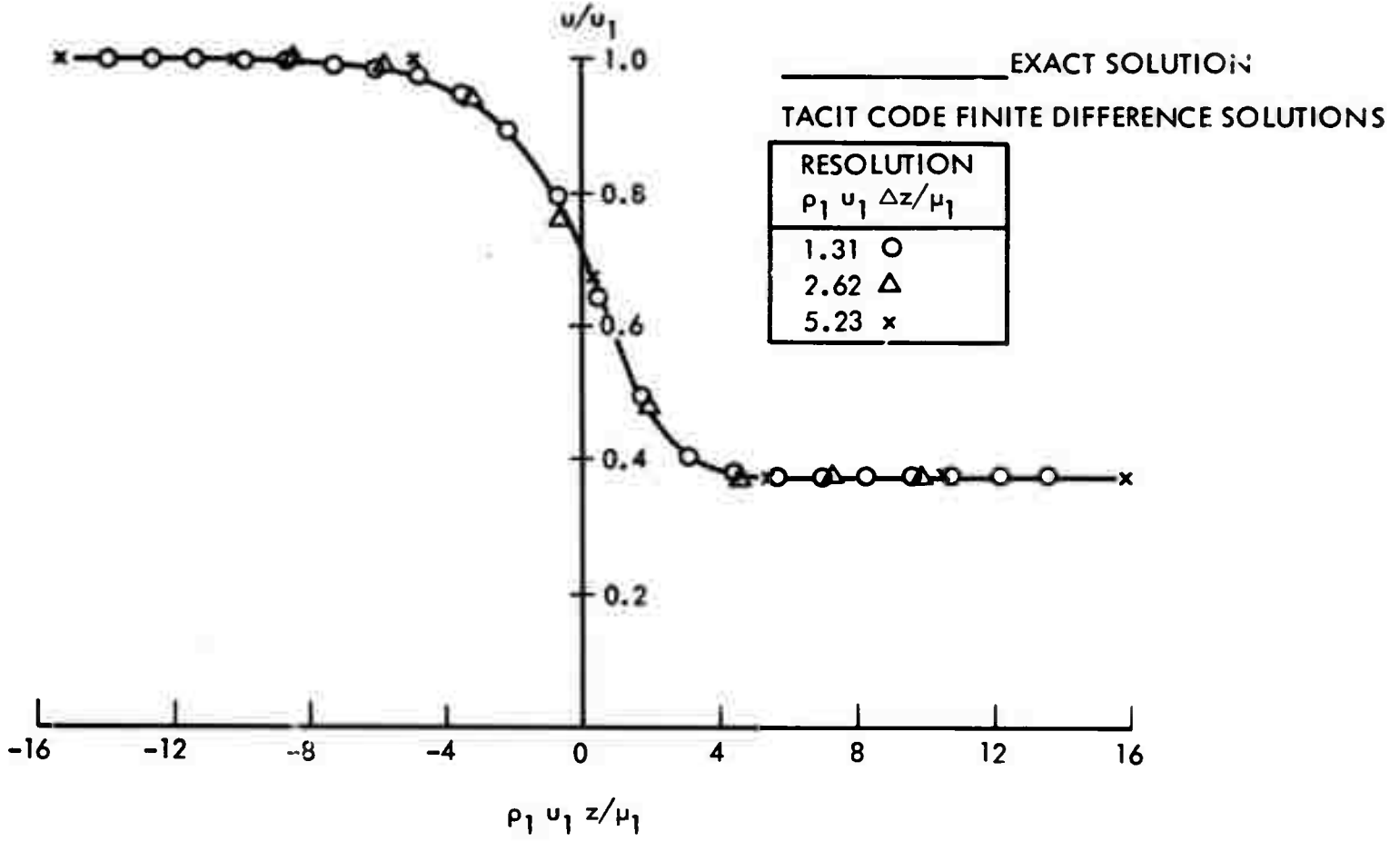

Figure 11. Effect of Spatial Resolution on Computed Shock Structure

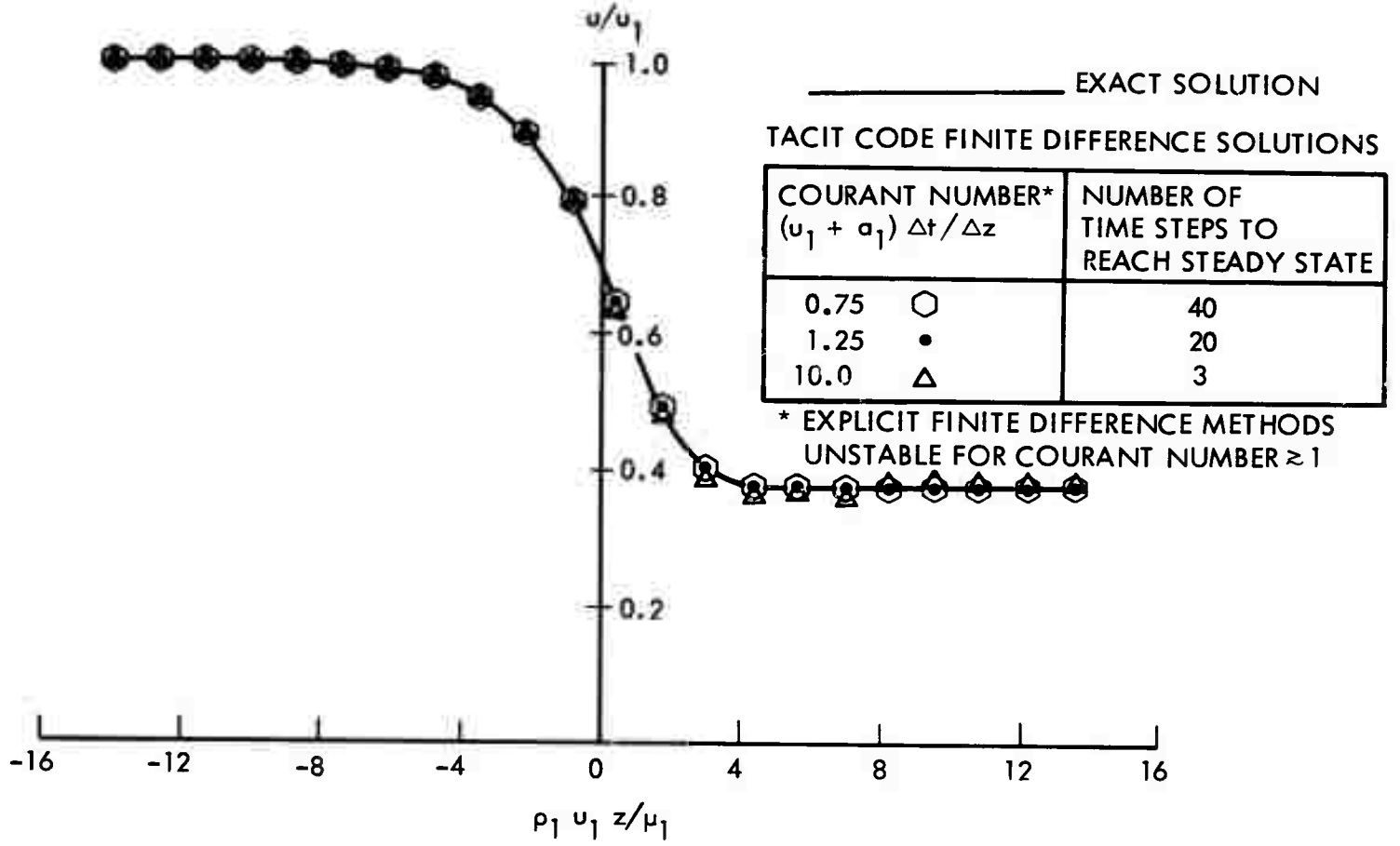

Figure 12. Effect of Temporal Step Size on Shock Structure Calculation

Since explicit difference methods are limited by stability considerations to $K_c \lesssim 1$, the calculation for $K_c = 10$ reaches a steady state in approximately one tenth the number of time steps required by an explicit method, with no significant degradation of the steady solution due to temporal truncation error. This, again, underlines the fundamental advantage of the implicit method, especially when the time dependent calculation is being used to obtain the asymptotic steady solution.

4. LAMINAR NEAR WAKE CALCULATION

A high Reynolds number slender body near wake calculation is under progress. The body is an 8 degree half-angle sharp cone, with $M_\infty = 21$, $Re_{\infty_D} = 7.8 \times 10^6$, $H_w/H_\infty = 0.02$ (cold wall). Under these conditions, the boundary layer at the rear of the body is expected to be fully turbulent. A steady calculation, using the methods of Reference 1, has previously been made for these conditions under the assumption that while the boundary layer profiles at the body shoulder correspond to boundary layer transition near the nose, the mixing in the near wake is dominated by the laminar viscosity. For the purpose of further testing the numerical techniques for the time-dependent calculation under conditions very close to those corresponding to the final (turbulent mixing) case, this calculation is being used as a test case for the laminar version of the code.

REFERENCES

1. Ohrenberger, J. T. and Baum, E., "A Theoretical Model of the Near Wake of a Slender Body in Supersonic Flow," AIAA Journal, Vol. 10, pp. 1165-1172, 1972.

2. Bradshaw, P., Ferriss, D. H., and Atwell, N. P., "Calculation of Boundary Layer Development using the Turbulent Energy Equation," Journal Fluid Mech., Vol. 28, Part 3, pp. 593-616, 1967.

3. Saffman, P. G., "A Model for Inhomogeneous Turbulent Flow," Proc. Roy. Soc. Lond. A, Vol. 317, pp. 417-433, 1970.

4. Jones, W. P. and Launder, B. E., "The Prediction of Laminarization with a Two-Equation Model of Turbulence," Int. Journal Heat Mass Transfer, Vol. 15, pp. 301-314.

5. Weighardt, K., Data presented in Proceedings Computation of Turbulent Boundary Layers - 1968, AF OSR-IFP, Stanford Conference, Vol. II, compiled Data, Ed. D. E. Coles and E. A. Hirst.

6. Klebanoff, P. S., "Characteristics of Turbulence in a Boundary Layer with Zero Pressure Gradient," NACA TN 3172, 1954.

7. Maise, G. and McDonald, H., "Mixing Length and Kinematic Eddy Viscosity in a Compressible Boundary Layer," AIAA Paper No. 67-199, Presented at AIAA 5th Aerospace Sciences Meeting, 1967.

8. Kistler, A. L., "Fluctuation Measurements in a Supersonic Turbulent Boundary Layer," Physics of Fluids, Vol. 2, No. 3, pp. 290-296, 1959.

9. Brailovskaya, I. Y., "A Difference Scheme for Numerical Solution of the Two-Dimensional, Nonstationary Navier-Stokes Equations for a Compressible Gas," Soviet Physics, Doklady, Vol. 10, pp. 107-110, 1965.

10. Victoria, K. and Steiger, M., "Exact Solution of the 2-D Laminar Near Wake of a Slender Body in Supersonic Flow at High Reynolds Number," Aerospace Corp. Report APP-0059(S9990)-5, October 1970.

11. Thommen, H. V., "Numerical Integration of Navier-Stokes Equations," ZAMP, Vol. 17, pp. 369-384, 1965.

12. Trulio, I. G., Wallitt, L., and Niles, W. J., "Numerical Calculations of Viscous Compressible Fluid Flow," Applied Theory Reports 68-5-1, 68-5-2, 68-5-3, 1968.

13. Harlow, F. H. and Amsden, A. A., "Numerical Calculation of Almost Incompressible Flow," Journal Computational Physics, Vol. 3, 80, 1968.

14. Godunov, S. K., Zabr odin, A. V., and Prokopov, G. D., "A Difference Scheme for a Two-Dimensional Unsteady Problem in Gas Dynamics and the Calculation of a Flow with a Detached Shock Wave," zh. Vychyslitelnye Material: Mathematic Fiziki 6, pp. 1020-1050, 1961.

15. Allen, J. S. and Cheng, S. I., "Numerical Solution of the Near Wake of Supersonic Flow with Boundary Layer Over a Sharp Corner," Physics of Fluids, Vol. 13, pp. 37-52, 1970.

16. Roache, P. J. and Mueller, T. J., "Numerical Solutions of Laminar Separated Flow," AIAA Journal, Vol. 8, pp. 530-538, 1970.

17. Peaceman, D. W. and Rachford, H. H., "The Numerical Solution of Parabolic and Elliptic Differential Equations," Journal Soc. Ind. Appl. Math Vol. 3 pp. 28-41, 1955.

18. Gourlay, A. R. and Mitchell, A. R., "A Stable Implicit Difference Method for Hyperbolic Systems in Two Space Dimensions," Numerische Mathematik 8, pp. 367-375, 1966.

19. Gary, J., "On Certain Finite Difference Schemes for Hyperbolic Systems," Math. of Computation 18, pp. 1-18, 1964.